

· 基础研究 ·

针刀干预对膝骨关节炎兔股直肌组织形态及超微结构的影响

刘晶¹, 林巧璇², 卢莉铭², 郭泽兴², 刘洪^{1,3}, 张良志^{1,3}, 修忠标^{1,3,4}

(1.福建中医药大学附属人民医院, 福建 福州 350004; 2.福建中医药大学中医学院, 福建 福州 350122; 3.中医骨伤及运动康复教育部重点实验室, 福建 福州 350122; 4.福建省骨伤研究所, 福建 福州 350004)

【摘要】 目的: 观察针刀干预对膝骨关节炎(knee osteoarthritis, KOA)兔股直肌组织形态及超微结构的影响, 揭示针刀治疗 KOA 可能的疗效机制。方法: 选取 6 月龄新西兰雄性兔 24 只, 体质量(2.0±0.5) kg, 采用随机数字表法分为空白组、模型组、针刀组, 每组 8 只。改良 Videman 法左后肢伸直位石膏固定制动 6 周复制 KOA 模型, 针刀组采用经筋理论指导下针刀松懈股四头肌经筋病灶点鹤顶穴、髌外上、髌内上治疗, 每周 1 次, 共治疗 4 次; 空白组和模型组正常饲养, 不干预。治疗结束后 1 周, 采用肌骨超声观察股直肌羽状角(pennation angle, PA), 肌肉厚度(muscle thickness, MT), 横截面积(cross-sectional area, CSA)及弹性应变率比值(atrain ratio, SR)的变化; HE 染色观察股直肌组织形态、肌纤维数量及平均横截面积的变化; 透射电镜观察股直肌组织肌原纤维、肌节和肌丝的超微结构变化。结果: 模型组股直肌 PA、MT 和 CSA 均较空白组小($P<0.05$), 针刀组较模型组大($P<0.05$)。模型组股直肌 SR 较空白组增大($P<0.05$), 针刀组较模型组减小($P<0.05$)。HE 染色结果显示, 空白组股直肌纤维排列整齐; 模型组股直肌肌束排列紊乱, 少量炎细胞浸润; 针刀组股直肌肌束排列趋于整齐, 炎细胞减少; 模型组在固定视野内肌纤维数量较空白组增加($P<0.05$), 平均横截面积较空白组减小($P<0.05$); 针刀组在固定视野内肌纤维数量较模型组减少($P<0.05$), 平均横截面积较模型组增加($P<0.05$)。电镜结果显示, 与空白组比较, 模型组股直肌纤维整体排列欠规整, Z 线断裂不连续; 与模型组比较, 针刀组股直肌纤维排列趋于整齐, Z 线较整齐。结论: 基于经筋理论针刀松懈股四头肌经筋病灶点能够有效改善 KOA 兔股直肌组织病理形态和结构, 促进骨骼肌慢性损伤的修复和重建, 这可能是针刀治疗 KOA 的作用机制之一。

【关键词】 膝骨关节炎; 针刀; 股直肌; 肌骨超声; 弹性成像; 电镜

中图分类号: R274.3

DOI: 10.12200/j.issn.1003-0034.2022.03.016

开放科学(资源服务)标识码(OSID):



Effect of acupotomy intervention on the morphology and ultrastructure of rectus femoris muscle in rabbits with knee osteoarthritis LIU Jing, LIN Qiao-xuan, LU Li-ming, GUO Ze-xing, LIU Hong, ZHANG Liang-zhi, and XIU Zhong-biao*. *The People's Hospital Affiliated of Fujian University of Traditional Chinese Medicine, Fuzhou 350004, Fujian, China*

ABSTRACT **Objective:** To observe the effect of acupotomy on the morphology and ultrastructure of rectus femoris muscle in rabbits with knee osteoarthritis and to reveal the possible therapeutic mechanism involved in the effect of acupotomy on the treatment of knee osteoarthritis (KOA). **Methods:** Twenty-four male New Zealand rabbits aged 6 months and weighed (2.0±0.5) kg were randomly divided into blank group, model group and acupotomy group, 8 rabbits in each group. KOA model was established by modified Videman method with left hind limb extended plaster immobilization for 6 weeks. In acupotomy group, the transverse focal points of quadriceps femoris muscle were released by acupotomy under the guidance of *Jingjin* theory for 4 times and once a week, and the treatment points include *Hedingci*, *Binwaixia*, *Binneixia*. Blank group and model group were fed normally without intervention. One week after the end of the intervention, the pennation angle (PA), muscle thickness (MT), cross-sectional area (CSA) and strain ratio (SR) of rectus femoris were measured by ultrasound. HE staining was used to observe the changes of the tissue morphology, the number of muscle fibers and the average area of muscle fibers. The myofibril of rectus femoris, sarcomere and myofilament were observed by transmission electron microscope. **Results:** The PA of rectus femoris muscle in the blank group was (9.05±0.21)°. The MT was (1.09±0.09) cm and the CSA was (1.30±0.01) cm². The PA of rectus femoris muscle in the model group was (3.06±0.15)°. The MT was (0.71±0.02) cm and the CSA was (0.77±0.02)

基金项目: 国家自然科学基金项目(编号: 81873315, 82004388); 福建省科技厅卫生联合面上项目(编号: 2019J01496); 国家中医临床研究基地专项科研课题(编号: JDZX201906)

Fund program: National Natural Science Foundation (NO. 81873315, 82004388)

通讯作者: 修忠标 E-mail: xzbdoctor@sina.com

Corresponding author: XIU Zhong-biao E-mail: xzbdoctor@sina.com

cm². The PA of rectus femoris muscle in the acupotomy group was (6.94±0.28)°. The MT was (0.80±0.05) cm and the CSA was (0.94±0.03) cm². The muscle PA, MT and CSA of rectus femoris in the model group were significantly smaller than those in the blank group ($P<0.05$). Those in acupotomy group were significantly increased compared with those in model group ($P<0.05$). The SR of rectus femoris muscle was 1.19±0.02 in the blank group, 3.50±0.05 in the model group and 1.99±0.07 in the acupotomy group. The elastic SR of the model group was significantly higher than that of the blank group ($P<0.05$). These in acupotomy group was significantly lower than that in model group ($P<0.05$). The results of HE staining showed: in blank group, the fascicles of rectus femoris were arranged neatly, the number of beam of muscle fibers within the fixed visual field was 94.38±3.50 and the average CSA was (0.75±0.22) mm². In model group, the fascicles of rectus femoris with different sizes were disorganized with a small amount of inflammatory cell infiltration, the number of beam of muscle fibers within the fixed visual field was 196.63±2.62 and the average CSA was (0.26±0.03) mm². Compared to the blank group, a significant increase in the number of muscle fibers in the fixed field in the model group ($P<0.05$) and the average CSA decreased significantly ($P<0.05$). In acupotomy group, the rectus femoris fascicles in the acupotomy group tended to be arranged in a more orderly manner, with the inflammatory cells decreased, the number of beam of muscle fibers within the fixed visual field was 132.88±4.61 and the average CSA was (0.70±0.07) mm². Compared to the model group, a significant decrease in the number of muscle fibers in the fixed field in the model group ($P<0.05$) and the average CSA increased significantly ($P<0.05$). The results of transmission electron microscope showed: compared with the blank group, the overall arrangement of the myofibrils of the rectus femoris in the model group was less structured. There was fracture between the muscle fibers and the sarcomere, the myofilaments were disordered, and the fracture of the Z line was discontinuous. Compared with the model group, the myofibrillar texture of rectus femoris in acupotomy group was clearer, and the Z line was more continuous. **Conclusion:** Based on the jingjin theory, the release of quadriceps femoris by acupotomy can effectively improve the morphology and structure of rectus femoris, and promote the repair and reconstruction of chronic skeletal muscle injury in rabbits with KOA, which may be one of the mechanisms of acupotomy in the treatment of KOA.

KEYWORDS Knee osteoarthritis; Acupotomy; Rectus femoris; Musculoskeletal ultrasound; Elastography; Electron microscope

膝骨关节炎(knee osteoarthritis, KOA)发病率、致残率较高,社会危害大。我国中老年人人群中症状性 KOA 患病率为 8.1%^[1],已成为全球第 4 大致残性疾病^[2],对 KOA 的防治研究具有重要意义。研究表明,基于经筋理论针刀松解膝周肌肉、韧带经筋病灶点能够调节骨骼肌功能,有效改善 KOA 患者疼痛和功能障碍^[3-5],然而,其作用机制尚不明确。近年来普遍认为 KOA 骨骼肌慢性损伤引起的筋骨失衡是导致 KOA 的重要机制之一^[6-7],调节骨骼肌功能,恢复筋骨平衡是改善 KOA 疼痛及功能障碍的有效途径^[8-9]。基于此,针刀治疗 KOA 的疗效可能与改善慢性损伤骨骼肌的组织形态及结构,调节骨骼肌功能有关。因此,本研究从股直肌的组织形态和超微结构等方面探讨针刀治疗 KOA 的可能作用,为临床针刀治疗 KOA 提供科学理论依据。

1 材料与方法

1.1 主要试剂与仪器

HE 染色试剂盒(北京索莱宝科技有限公司),10%水合氯醛(上海阿拉丁生化科技股份有限公司),75%乙醇、碘伏消毒剂、4%多聚甲醛、10%EDTA、0.9%NaCl 注射液(均购自南京丁贝生物有限公司),5%戊二醛(福建省中医药研究院实验动物中心提供)。一次性使用无菌 0.4 mm×40 mm 小针刀(江西老宗医医疗器械有限公司),DR 机(日本岛津),3.0 T

高场强核磁共振(德国西门子),光学显微镜、自动脱水机、组织包埋机、Leica 2025 石蜡切片(德国 Leica 公司),透射电子显微镜(日立 HT7700),高分子石膏(陕西安信医学技术开发有限公司),普通石膏(浦江健宇卫生材料有限公司生产),手术刀片及相关器械(均购自上海医疗器械批发部有限公司),一次性包埋盒、包埋模具(均购自上海源叶生物技术有限公司),粘附载玻片、盖玻片(均购自江苏世泰实验器材有限公司)。

1.2 实验动物及分组

普通级健康雄性 6 月龄新西兰大白兔 24 只,体质量(2.0±0.5)kg,由上海松联实验动物责任有限公司提供,动物合格证号为 SCXK(沪)2017-0008。委托福建省中医药研究院实验动物中心 [SYXK(闽)2016-0005]饲养。实验动物单笼喂养,饲养房温度 20~25℃,湿度 30%~60%,自然光照,自由进食、饮水。适应性饲养 1 周后,按照体质量进行编号,并应用随机数字表法将其分为空白组、模型组、针刀组,每组 8 只。本实验已通过福建省中医药研究院动物实验伦理委员会批准(编号:FJATCM-IAEC2019 037),实验过程对动物的处置遵循科技部颁布的《关于善待实验动物的指导性意见》相关规定。

1.3 造模方法

参照改良 Videman 法将兔子仰卧于固定架

上^[10],膝前放置石膏托,高分子石膏绷带单层螺旋缠绕,保持膝关节伸直中立位 0°,踝关节背曲 60°,最后使用防啃咬绷带环形缠绕高分子石膏表面。固定 6 周后 Lequesne MG 膝关节级别评分增高,X 线和 MRI 影像学检测示关节间隙变窄、软骨面欠光滑为模型成功。

1.4 干预措施

空白组和模型组只做同样的抓取和固定,不予针刀治疗。针刀组:造模成功 1 周后进行针刀干预,依据《中国经筋学》^[11] 膝关节经筋病灶点命名及定位,根据兔的骨度分寸,选取治疗点鹤顶次(股四头肌肌腱髌骨正上缘附着处),髌外上(股外侧肌肌腱髌骨外上缘附着处),髌内上(股内侧肌肌腱髌骨内上缘附着处)。在施术部位,用活力碘消毒 3 遍,然后铺无菌洞巾,使治疗点正对洞巾中间。术者戴好无菌手套,采用 0.4 mm×40 mm 针刀进行松解,刀口线垂直皮肤进针刀,针刀抵达病变处骨面,行提插刀法松解,范围不超过 0.5 cm。操作结束后用无菌干棉球在手术部位按压 1 min。每 7 d 干预 1 次,干预 4 次。

1.5 检测指标与方法

1.5.1 肌骨超声测量 针刀干预结束后 1 周,采用腹腔注射 10%水合氯醛溶液(3 ml/kg)麻醉实验兔,行左膝关节超声检测^[12]。高频超声成像:使用 EPIQ7 超声诊断仪器,选取肌肉骨骼超声模式,运用高频线阵探头(5~18 MHz)在髌上 2 cm 股直肌正中处进行短轴和长轴成像,反复测量 3 次。测量指标:(1)羽状角(pennation angle, PA)。在高频超声长轴图像中根据股直肌肌束的排列方向和深层肌腱膜的方向可以画出肌束线和深层肌腱膜线,两线的夹角即为羽状角,测量羽状角大小。(2)肌肉厚度(muscle thickness, MT):在高频超声长轴图像中测量股直肌浅筋膜与深筋膜的的距离。(3)肌肉周长和横截面积(cross-sectional area, CSA):在高频超声短轴图像中测量股直肌周长和横断面积。弹性成像:运用高频线阵探头(5~18 MHz)在髌上 2 cm 股直肌正中处长轴成像,当出现清晰图像后,选取弹性成像模式,进行弹性成像,反复测量 3 次。采用超声弹性成像分析软件分析弹性成像图,计算股直肌的弹性应变率比值(atrain ratio, AR)。弹性应变率比值=股直肌感兴趣点/皮下组织的应变值。

1.5.2 HE 染色观察 针刀干预结束后 1 周,麻醉下耳缘静脉空气栓塞处死,迅速解剖左侧膝关节,行髌前正中切口,逐层分离至关节囊,用尖刀切断股四头肌在髌骨上缘附着处肌腱,分离股直肌,迅速取髌上 2~3 cm 股直肌,用生理盐水清洗、滤纸吸干后,投入 4%多聚甲醛中固定 24 h,固定后用流水冲洗标本

4 h,脱水、包埋,以厚度 5 μm 制备组织切片。HE 染色:将组织切片置于 60 °C 烘箱中干燥 30 min 后,放入二甲苯中脱蜡 10 min;然后梯度乙醇溶液中入水各 3 min;沥干后浸入苏木精液中染色 15 min,蒸馏水冲洗;1%盐酸乙醇分色 3 s,流水冲洗 20 min 至水清澈;磷酸盐缓冲盐水(phosphate buffered saline, PBS)返蓝,蒸馏水冲洗;入伊红染料复染 30 s,使细胞质染成红色,中性树胶封片,待封片剂凝固后拍照。染色完成的肌肉 HE 切片在光学显微镜下进行观察,并使用 Image J 软件进行分析,固定视野下肌纤维数和肌纤维平均横截面积分别进行统计学分析。

1.5.3 透射电镜观察 5%的戊二醛固定样品 24 h 以上;磷酸缓冲液清洗样品,1%锇酸固定 1.5 h,蒸馏水清洗;乙醇逐级脱水;纯树脂包埋过夜;纯树脂包埋置烘箱;超薄切片,釉染色 5 min,水洗后铅染色 5 min,水洗;上机观察(日立 HT7700 透射电子显微镜)兔股直肌肌原纤维及肌节等超微结构。

1.6 统计学处理

采用 SPSS 20.0 软件进行统计学分析。定量资料数据以均数±标准差($\bar{x}\pm s$)表示,3 组间比较采用单因素方差分析,组间多重比较采用 LSD-*t* 检验。以 $P<0.05$ 为差异有统计学意义。

2 结果

2.1 股直肌超声声像图特征及各测量指标的比较

空白组股直肌超声声像为低回声中均匀的点状高回声,肌纤维排列整齐,肌束膜和肌外膜轮廓清晰,弹性成像呈绿色为主的低弹性图。模型组股直肌超声声像为低回声中出现不均匀片状高回声,肌纤维排列紊乱,肌束膜、肌外膜轮廓模糊,弹性成像呈红色为主的高弹性图。针刀组股直肌超声声像为低回声中稍不均匀的点状高回声,肌纤维排列、肌束膜和肌外膜轮廓趋于正常,弹性成像呈黄绿色为主的中弹性图。与空白组比较,针刀组和模型组羽状角、肌肉厚度及横截面积减小($P<0.05$),弹性应变率比值增大($P<0.05$);与模型组比较,针刀组羽状角、肌肉厚度及横截面积增加($P<0.05$),弹性应变率比值减小($P<0.05$)。见图 1,表 1。

2.2 股直肌 HE 染色形态学变化

与空白组比较,针刀组和模型组股直肌 HE 染色在固定视野内(10 μm×20 μm)肌纤维数量显著增加($P<0.05$),平均横截面积显著减少($P<0.05$);与模型组比较,HE 染色在固定视野内(10 μm×20 μm)肌纤维数量显著减少($P<0.05$),平均横截面积显著增加($P<0.05$)。见图 2,表 2。

2.3 股直肌透射电镜超微结构变化

空白组股直肌纤维排列整齐有序,肌节结构完

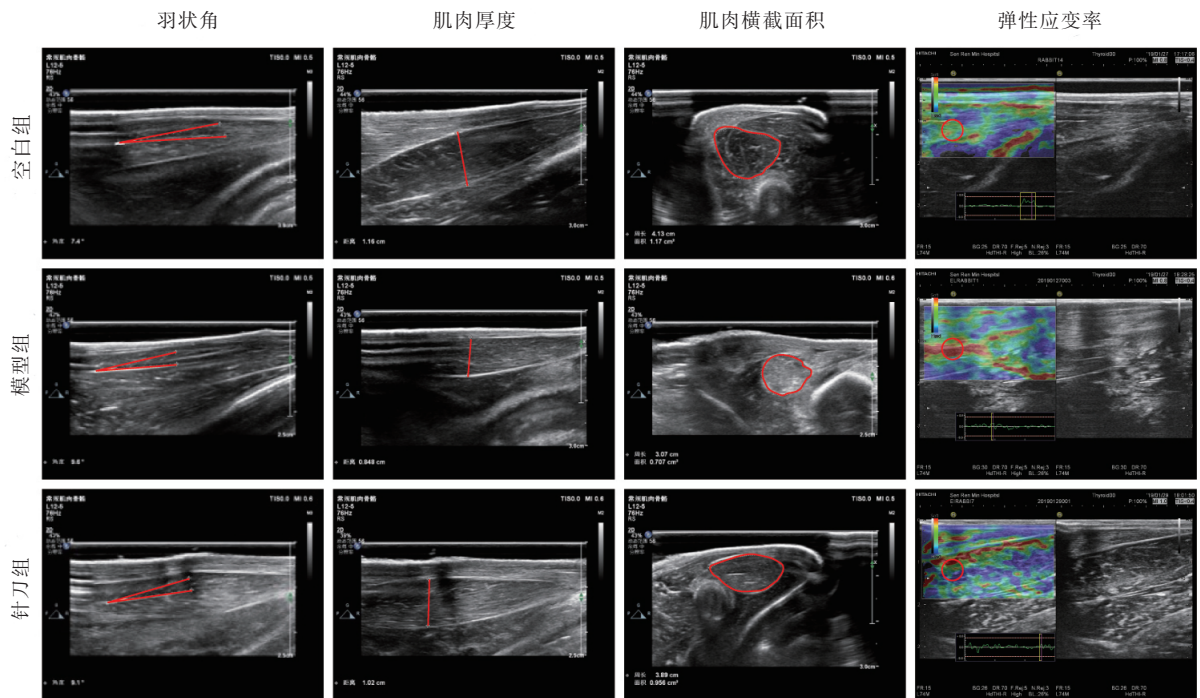


图 1 各组兔股直肌羽状角、肌肉厚度、横截面积及弹性超声声像图。各组兔股直肌羽状角、肌肉厚度、横截面积:空白组>针刀组>模型组;弹性应变率图像中圆圈示股直肌感兴趣点(距髌骨正上缘 2 cm)的弹性色图,空白组为绿色,模型组为红色,针刀组为黄色;弹性应变率比值:模型组>针刀组>空白组

Fig.1 Elastic ultrasonography of the muscle pennation angle, muscle thickness, muscle cross-sectional area and elastic strain of rectus femoris in three groups of rabbits. Comparison of pennation angle, muscle thickness and cross-sectional area of rectus femoris in three groups: blank group > acupotomy group > model group; In the elastic strain rate image, the circle shows the elastic color map of the interest point of rectus femoris (2 cm from the right edge of the patella), and the blank group was green, the model group was red, and the acupotomy group was yellow. The ratio of elastic strain rate of the three groups was compared: model group > acupotomy group > blank group

表 1 各组兔股直肌羽状角、肌肉厚度、横截面积、股直肌弹性应变率比较($\bar{x}\pm s$)

Tab.1 Comparison of the feather angle, muscle thickness and cross-sectional area, elastic strain rate of rabbit rectus femoris in each group($\bar{x}\pm s$)

| 组别 | 兔数 | 羽状角(°) | 肌肉厚度(cm) | 横截面积(cm ²) | 弹性应变率 |
|-----|----|----------------------------|----------------------------|----------------------------|----------------------------|
| 空白组 | 8 | 9.05±0.21 | 1.09±0.09 | 1.30±0.01 | 1.19±0.02 |
| 模型组 | 8 | 3.06±0.15 ^{a1} | 0.71±0.02 ^{a3} | 0.77±0.02 ^{a5} | 3.50±0.05 ^{a7} |
| 针刀组 | 8 | 6.94±0.28 ^{a2/b1} | 0.80±0.05 ^{a4/b2} | 0.94±0.03 ^{a6/b3} | 1.99±0.07 ^{a8/b4} |
| F 值 | | 1525.558 | 88.496 | 1170.469 | 3504.352 |
| P 值 | | <0.001 | <0.001 | <0.001 | <0.001 |

注:与空白组相比,^{a1} $t=54.452, P=0.000$;^{a2} $t=19.191, P=0.000$;^{a3} $t=11.875, P=0.000$;^{a4} $t=8.067, P=0.000$;^{a5} $t=47.463, P=0.000$;^{a6} $t=31.866, P=0.000$;^{a7} $t=-82.409, P=0.000$;^{a8} $t=-28.434, P=0.000$ 。与模型组相比,^{b1} $t=-35.262, P=0.000$;^{b2} $t=-4.852, P=0.000$;^{b3} $t=-15.596, P=0.000$;^{b4} $t=53.975, P=0.000$

Note: Compared with the blank group, ^{a1} $t=54.452, P=0.000$; ^{a2} $t=19.191, P=0.000$; ^{a3} $t=11.875, P=0.000$; ^{a4} $t=8.067, P=0.000$; ^{a5} $t=47.463, P=0.000$; ^{a6} $t=31.866, P=0.000$; ^{a7} $t=-82.409, P=0.000$; ^{a8} $t=-28.434, P=0.000$. Compared with the model group, ^{b1} $t=-35.262, P=0.000$; ^{b2} $t=-4.852, P=0.000$; ^{b3} $t=-15.596, P=0.000$; ^{b4} $t=53.975, P=0.000$

整,Z 线连续无断裂。模型组股直肌纤维排列紊乱无序,部分肌纤维断裂、破损,肌节结构破坏,Z 线断裂不连续。针刀组股直肌纤维恢复有序状态,肌纤维较完整,Z 线较整齐。见图 3。

3 讨论

3.1 针刀循股四头肌经筋病灶点松解对 KOA 兔股直肌组织形态和弹性的影响

本研究结果显示,造模后,模型组股直肌模型组羽状角、肌肉厚度及横截面积显著减小,弹性应变率比值显著增大;肌束排列紊乱,少量炎细胞浸润,肌纤维数量增加,平均横截面积减少。针刀干预后股直肌羽状角、肌肉厚度及横截面积增大,弹性应变率比值减小;肌束排列趋于整齐,炎细胞减少,肌纤维数量显著减少,平均横截面积显著增加。这表明在 KOA 兔模型中,长期异常机械应力下出现骨骼肌慢性损伤,表现为肌肉炎症

反应、萎缩、肌纤维紊乱、组织硬度增加。通过针刀对股四头肌经筋病灶点组织的针刺和切割,有效释放肌肉组织的张力,改善肌肉生物力学环境,有效消除了 KOA 兔股直肌肌肉的炎症,减轻肌肉萎缩状态,

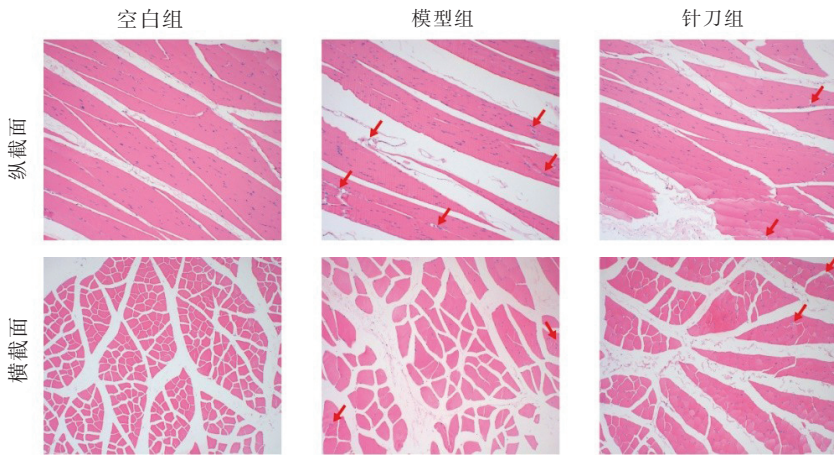


图 2 3 组兔股直肌 HE 染色病理改变情况($\times 100$)。红色箭头示炎症细胞浸润。空白组股直肌纵切面肌纤维排列整齐,肌细胞均匀分布;横截面示肌束大小匀称。模型组股直肌纵切面肌纤维排列紊乱,少量炎细胞浸润;横截面示肌束大小不一,纤维数量减少。针刀组股直肌纵切面肌纤维排列趋于整齐,肌细胞分布较均匀,炎细胞减少;横截面示纤维数量增多

Fig.2 Changes of the HE staining of rectus femoris in three groups of rabbits ($\times 100$). The red arrows indicate infiltration of inflammatory cells. In the blank group, the muscle fibers of rectus femoris in longitudinal section were arranged neatly and the muscle cells were evenly distributed, and the cross section shows the well-proportioned fascicles. In the model group, the longitudinal section of rectus femoris muscle fiber arrangement was disordered and a few inflammatory cells infiltrated, and the muscle bundles had varying sizes across the cross section and the number of fibers is reduced. In the acupotomy group, the muscle fibers of the rectus femoris in longitudinal section tended to be arranged neatly, the distribution of muscle cells was more uniform, and the inflammatory cells were reduced, and the cross section shows an increase in the number of fibers

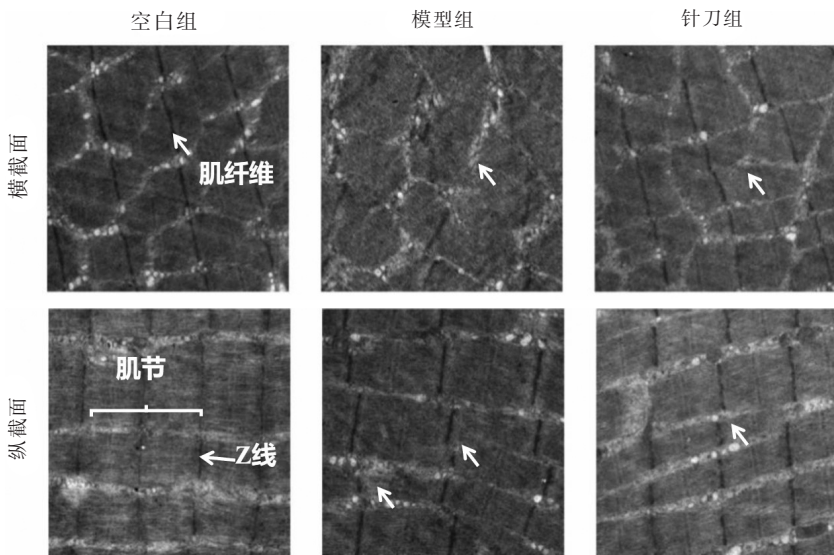


图 3 3 组兔股直肌电镜下横截面、纵截面肌原纤维、肌节变化情况。空白组箭头示肌纤维排列整齐,肌节结构完整,Z 线连续。模型组箭头示肌纤维排列紊乱无序,肌节结构破坏,Z 线断裂不连续。针刀组箭头示肌纤维排列稍紊乱,肌节结构较完整,Z 线稍扭曲

Fig.3 Changes of myofibrils, sarcomere and myofilament in cross section and longitudinal section under electron microscope of rectus femoris in three groups of rabbits. In the blank group, the arrows showed that the muscle fibers were neatly arranged, the sarcomere structure was intact, and the Z-line was continuous. In the model group, the arrows showed the disordered arrangement of muscle fibers, the destruction of muscle node structure, and the Z-line fracture discontinuity. In the acupotomy group, the arrows showed slightly disordered arrangement of muscle fibers, relatively complete sarcomere structure, and slightly distorted Z line

降低肌肉组织硬度。其他学者研究也显示针刀能够促进股四头肌纤维化修复,提高股四头肌收缩能力,调整膝关节肌腱、韧带生物力学性能^[13-14]。可见,基于经筋理论针刀循股四头肌经筋病灶点松解能有效修复和调节 KOA 兔股直肌组织病理形态和组织硬度。

3.2 针刀循股四头肌经筋病灶点松解对 KOA 兔股直肌组织超微结构的影响

本研究结果显示, KOA 兔股直肌纤维排列紊乱无序,部分肌纤维断裂、破损,Z 线断裂不连续。针刀组干预后股直肌纤维恢复有序状态,肌纤维较完整,Z 线较整齐。表明在 KOA 兔模型中,股直肌慢性损伤后出现肌节结构破会和肌丝排列紊乱,针刀松解股四头肌经筋病灶点能够恢复较正常的肌节结构和肌丝排列。其作用机制可能包括:(1) 针刀能够通过微小损伤产生良性的炎症反应,激活人体修复系统,同时改善股直肌病损部位的血液循环,促进肌纤维的修复。(2) 针刀能调整股直肌病损部位的异常机械应力,恢复肌肉的适宜长度,从而调节肌节结构和恢复肌丝排列。基于此,经筋理论指导下针刀循股四头肌经筋病灶点松解能促进 KOA 兔股直肌组织超微结构的损伤修复。

综上所述,改良 Videman 法制备 KOA 兔模型中股直肌慢性损伤出现组织形态和超微结构的改变,基于经筋理论针刀松解股四头肌经筋病灶点能够有效改善股直肌组织形态和超微结构,促进 KOA 兔骨骼肌慢性损伤的修复和重建。但本研究仍存在以下不足:(1) 未对不同时期 KOA 兔模型的针刀干预对股直肌的组织形态和超微结构的影响进行评价。(2) 未对 KOA 兔模型股直肌的组织形态和超微结构的改变与膝关节功能相关性进行分析。

表 2 各组兔股直肌肌纤维数量及肌纤维平均面积比较($\bar{x}\pm s$)

Tab.3 Comparison of the number of muscle fibers and the average area of muscle fibers in each group of rabbit rectus femoris($\bar{x}\pm s$)

| 组别 | 兔数 | 肌纤维数量(束) | 肌纤维平均面积(mm ²) |
|-----|----|-----------------------------|---------------------------|
| 空白组 | 8 | 94.38±3.50 | 0.75±0.22 |
| 模型组 | 8 | 196.63±2.62 ^{a1} | 0.26±0.03 ^{a3} |
| 针刀组 | 8 | 132.88±4.61 ^{a2b1} | 0.70±0.07 ^{a4b2} |
| F 值 | | 1585.276 | 32.541 |
| P 值 | | <0.001 | <0.001 |

注：与空白组相比，^{a1}t=-55.744, P=0.000; ^{a2}t=-20.989, P=0.000; ^{a3}t=-113.492, P=0.000; ^{a4}t=-27.590, P=0.000。与模型组相比，^{b1}t=34.755, P=0.000; ^{b2}t=45.445, P=0.000

Note: Compared with the blank group, ^{a1}t=-55.744, P=0.000; ^{a2}t=-20.989, P=0.000; ^{a3}t=-113.492, P=0.000; ^{a4}t=-27.590, P=0.000. Compared with the model group, ^{b1}t=34.755, P=0.000; ^{b2}t=45.445, P=0.000

参考文献

[1] Tang X, Wang S, Zhan S, et al. The prevalence of symptomatic knee osteoarthritis in China: results from China health and retirement longitudinal study[J]. Arthritis Rheum, 2016, 68(3): 648-653.

[2] Cross M, Smith E, Hoy D, et al. The global burden of hip and knee osteoarthritis: estimates from the global burden of disease 2010 study[J]. Ann Rheum Dis, 2014, 73(7): 1323.

[3] 刘建民, 刘晶. 从经筋弓弦特性探析针刀治疗膝骨性关节炎[J]. 中国医药导报, 2017, 14(27): 161-164.

LIU JM, LIU J. Exploration on the acupotomy therapy for knee osteoarthritis from the characteristics of aponeurotic system and bowstring[J]. Zhongguo Yi Yao Dao Bao, 2017, 14(27): 161-164. Chinese.

[4] 修忠标, 张春霞, 刘洪, 等. 针刀治疗膝骨性关节炎临床观察及机制探讨[J]. 辽宁中医药大学学报, 2018, 20(1): 15-18.

XIU ZB, ZHANG CX, LIU H, et al. Clinical effect observation and mechanism discussion on needle knife release in treatment of knee osteoarthritis[J]. Liao Ning Zhong Yi Yao Da Xue Xue Bao, 2018, 20(1): 15-18. Chinese.

[5] 胡波, 于佳妮, 张慧方, 等. 针刀干预对 KOA 兔关节软骨病理学及股四头肌收缩性能的影响[J]. 针灸临床杂志, 2018, 34(11): 50-54.

HU B, YU JN, ZHANG HF, et al. Effect of acupotomy intervention on contractility of quadriceps femoris and pathological changes of articular cartilage in KOA rabbits[J]. Zhen Jiu Lin Chuang Za Zhi, 2018, 34(11): 50-54. Chinese.

[6] 张洪美. 膝骨性关节炎的规范诊治与阶梯治疗[J]. 中国骨伤,

2019, 32(5): 391-395.

ZHANG HM. Standardized diagnosis-therapy and stepwise treatment for knee osteoarthritis[J]. Zhongguo Gu Shang/China J Orthop Trauma, 2019, 32(5): 391-395. Chinese.

[7] Bandak E, Boesen M, Bliddal HA, et al. Associations between muscle perfusion and symptoms in knee osteoarthritis: across sectional study[J]. Osteoarthritis Cartilage, 2015, 23(10): 1721-1727.

[8] Francisco V, Perez T, Pion J, et al. Biomechanics, obesity, and osteoarthritis. The role of adipokines: when the levee breaks[J]. J Orthop Res, 2018, 36(2): 594-604.

[9] 李西海, 刘献祥. 基于筋骨理论探讨膝骨关节炎筋骨失衡的治疗策略[J]. 中华中医药杂志, 2017, 32(8): 3344-3346.

LI XH, LIU XX. Treatment strategy of knee osteoarthritis with Jin-Gu imbalance based on the Jin-Gu theory[J]. Zhonghua Zhong Yi Yao Za Zhi, 2017, 32(8): 3344-3346. Chinese.

[10] 刘晶, 林巧璇, 卢莉铭, 等. 改良 Videman 法复制兔膝关节关节炎的实验研究[J]. 康复学报, 2020, 30(3): 212-219.

LIU J, LIN QX, LU LM, et al. Experimental study of modified videman method to replicate knee osteoarthritis in rabbits[J]. Kang Fu Xue Bao, 2020, 30(3): 212-219. Chinese.

[11] 薛立功. 中国经筋学[M]. 北京: 中医古籍出版社, 2009: 681-728.

XUE LG. Zhongguo Jing Jin Xue[M]. Beijing: Chinese Medicine Ancient Books Publishing House, 2009: 681-728. Chinese.

[12] 刘晶, 林巧璇, 宫玉榕, 等. 超声多模态联合技术评估膝骨性关节炎兔股直肌病变的应用探析[J]. 中国医药导报, 2020, 17(7): 147-151.

LIU J, LIN QX, GONG YR, et al. Discussion on application of ultrasonic multimodal combined technique in the evaluation of femoral rectus in rabbits with knee osteoarthritis[J]. Zhongguo Yi Yao Dao Bao, 2020, 17(7): 147-151. Chinese.

[13] 梁楚西, 陶琳, 肖红, 等. 针刀干预对 KOA 兔内侧副韧带生物力学特性及软骨 Integrin $\beta 1$ 、Col-II 基因表达的影响[J]. 中华中医药杂志, 2015, 30(5): 1689-1693.

LIANG CX, TAO L, XIAO H, et al. Effects of acupotomy therapy on biomechanical properties of medial collateral ligament and integrin $\beta 1$, Col-II mRNA of cartilage in rabbits with knee osteoarthritis[J]. Zhonghua Zhong Yi Yao Za Zhi, 2015, 30(5): 1689-1693. Chinese.

[14] 王丽娟, 史晓伟, 张伟, 等. 针刀干预对膝骨关节炎兔股四头肌肌腱拉伸力学的影响[J]. 中国骨伤, 2019, 32(5): 462-468.

WANG LJ, SHI XW, ZHANG W, et al. Effect of needle knife intervention on tensile mechanics of femoral quadriceps tendon in rabbits with knee osteoarthritis[J]. Zhongguo Gu Shang/China J Orthop Trauma, 2019, 32(5): 462-468. Chinese with abstract in English.

(收稿日期: 2020-11-17 本文编辑: 李宜)